Kinetics and Thermochemistry of the Reversible Combination Reactions of the Allyl and Benzyl Radicals with NO

ARTICLE *in* THE JOURNAL OF PHYSICAL CHEMISTRY · APRIL 1995

Impact Factor: 2.78 · DOI: 10.1021/j100027a022

3 AUTHORS, INCLUDING:

Barbara Noziere
French National Centre for Scientific Resea…

56 PUBLICATIONS **1,090** CITATIONS

SEE PROFILE

Reprinted from The Journal of Physical Chemistry, 1995, 99.

Kinetics and Thermochemistry of the Reversible Combination Reactions of the Allyl and Benzyl Radicals with NO

A. A. Boyd, B. Nozière, and R. Lesclaux*

Laboratoire de Photophysique et de Photochimie Moléculaire, URA 348 CNRS, Université Bordeaux I, 33405 Talence Cedex, France

Received: February 14, 1995; In Final Form: May 5, 1995[⊗]

The equilibrium kinetics of the reversible additions of NO to the benzyl ($C_6H_5CH_2$) and allyl (CH_2CHCH_2) radicals have been studied at atmospheric pressure and over the temperature range $400 < T < 520$ K. Experiments were performed using a flash photolysis/UV absorption technique with kinetic data being derived from numerical simulation of real-time decays of benzyl and allyl radicals, recorded both with and without the addition of excess nitric oxide. The equilibrium constants were therefore deduced as the ratio of the rate coefficients (k_1/k_{-1} and k_3/k_{-3}) for the forward and reverse processes: $C_6H_5CH_2 + NO + N_2 \leftrightarrow C_6H_5CH_2NO + N_2$ (reactions 1, −1) and $CH_2CHCH_2 + NO + N_2 \leftrightarrow CH_2CHCH_2NO + N_2$ (reactions 3, −3). Thermodynamic treatment of the data by both second law and third law methods of analysis yielded values for the enthalpy and entropy of reactions 1 and 3 which were self-consistent and hence the following average values: reaction 1, $\Delta H°_{298} = -123 \pm 5$ kJ mol^{-1} (thus $\Delta H°_0 = -117 \pm 6$ kJ mol^{-1} and $\Delta H_f°_{298}(C_6H_5CH_2NO) = 176 \pm 7$ kJ mol^{-1}, $\Delta S°_{298} = -159 \pm 9$ J K^{-1} mol^{-1}); reaction 3, $\Delta H°_{298} = -110 \pm 5$ kJ mol^{-1} (thus $\Delta H°_0 = -105 \pm 4$ kJ mol^{-1} and $\Delta H_f°_{298}$ (CH_2CHCH_2NO) = 148 ± 8 kJ mol^{-1}, $\Delta S°_{298} = -154 \pm 9$ kJ mol^{-1}). The bond dissociation energies for these adducts ($= -\Delta H°_{298}$) are compared and discussed in relation to those for other alkyl nitrosos. Also as part of the study, some measurements of the rate coefficients for the benzyl and allyl association reactions with NO (reactions 1 and 3) and their radical self-recombinations (reaction 4, $C_6H_5CH_2 + C_6H_5CH_2$, and reaction 5, $CH_2CHCH_2 + CH_2CHCH_2$) were made under similar experimental conditions, yielding (in units 10^{-11} cm^3 molecule^{-1} s^{-1}): k_1(415, 443, 466 K) = 0.91 ± 0.08, 0.81 ± 0.05, and 0.62 ± 0.09, k_3(403 K) = 0.71 ± 0.04, k_4(435−519 K) = 2.9 ± 0.3, k_5(403−540 K) = 2.6 ± 0.2.

Introduction

Addition and recombination processes involving organic free radicals (R) are not only of fundamental kinetic importance but also in an applied sense, being important intermediate steps in the tropospheric oxidation and higher temperature combustion of hydrocarbons. Even under polluted tropospheric conditions corresponding to relatively high NO_x concentrations, R is rapidly converted to RO_2 (rather than RNO or RNO_2) and thus the reactive peroxy radical has a much more important role to play in atmospheric chemistry.[1] However, the relative stability of nitroso compounds means that NO can be added to chemical systems where a scavenger is required for organic radicals, such as in laboratory studies of hydrocarbon decomposition mechanisms.[2] At only moderately elevated temperatures, peroxy and nitroso species can become unstable toward reactant reformation and a knowledge of the relevant equilibrium constants is then important in determining changes in the concentrations of R and of the adduct under certain experimental conditions, as well as helping to improve our understanding of the thermochemistry of such reactions. Of particular recent interest have been the kinetics of methyl and halogenated methyl radicals in their temperature- and pressure-dependent reactions with oxygen and nitrogen monoxide, forming peroxy (RO_2) and nitroso (RNO) adducts.[3-7] However, similar systems involving the important conjugated organic radicals benzyl ($C_6H_5CH_2$) and allyl (CH_2CHCH_2) have been less extensively studied, in particular their combination reactions with NO.

Ebata *et al.*[8] first investigated the kinetics of the reaction

$$C_6H_5CH_2 + NO + M \rightarrow C_6H_5CH_2NO + M \quad (1)$$

using a flash photolysis/UV absorption apparatus and $C_6H_5CH_2Br$ to produce benzyl radicals in the presence of excess NO, measuring $k_1 = 9.5 \times 10^{-12}$ cm^3 molecule^{-1} s^{-1} ($T = 298$ K, $P = 0.14$−200 Torr, M = N_2). Rate coefficients of around this value have since been measured[9] but for substituted benzyl radicals which could be monitored by laser induced fluorescence in a discharge-flow apparatus. We recently published kinetic data for the addition reaction

$$C_6H_5CH_2 + O_2 + M \rightarrow C_6H_5CH_2O_2 + M \quad (2)$$

obtained as a function of temperature using the laser photolysis technique.[10] The same paper also describes how results obtained from a flash photolysis technique indicate that the reverse dissociation process

$$C_6H_5CH_2O_2 + M \rightarrow C_6H_5CH_2 + O_2 + M \quad (-2)$$

becomes important under readily accessible conditions (P = 760 Torr, $T = 398$−525 K, M = N_2) and thus how the equilibrium constant and hence thermochemical and RRKM parameters can be derived for reaction 2.

The only study to date of the equivalent allyl association reaction

$$CH_2CHCH_2 + NO + M \rightarrow CH_2CHCH_2NO + M \quad (3)$$

is that of Tulloch *et al.*,[11] who used both laser and flash photolysis kinetic techniques, incorporating allyl radical detection by UV absorption, and observed a distinct temperature and pressure dependence for k_3 over the range $T = 295$−400 K, P

* Author to whom correspondence should be addressed.
[⊗] Abstract published in *Advance ACS Abstracts,* June 15, 1995.

0022-3654/95/2099-10815$09.00/0

= 50−500 Torr. The same group had also previously observed and quantified the association and dissociation kinetics for the equilibrium system involving allyl radicals and molecular oxygen.[12,13]

We present in this paper the first experimental evidence for the equilibrium reactions of benzyl and allyl radicals with NO:

$$C_6H_5CH_2 + NO + M \leftrightarrow C_6H_5CH_2NO + M \quad (1, -1)$$

$$CH_2CHCH_2 + NO + M \leftrightarrow CH_2CHCH_2NO + M \quad (3, -3)$$

The equilibrium constants, K_c, have been measured as a function of temperature, where the respective K_c values (given by the ratio k_1/k_{-1} or k_3/k_{-3}) were determined from kinetic simulations of benzyl or allyl radical decay traces recorded under equlibrium conditions using the flash photolysis technique (T = 435−520 K for benzyl and 403−473 K for allyl, P = 760 Torr and M = N_2). Second law and third law thermodynamic analyses then allow the enthalpy and entropy changes, $\Delta H°_{298}$ and $\Delta S°_{298}$, to be calculated for reactions 1 and 3. In addition, some initial kinetic studies of the benzyl and allyl reaction systems were performed at selected temperatures and NO concentrations where the association and dissociation components of the decay could be separated during the approach to equilibrium. Such experiments yield high-pressure limiting rate coefficients for reactions 1 and 3, to complement those measured at lower pressures.[8,11] The kinetics of the radical recombination reactions

$$C_6H_5CH_2 + C_6H_5CH_2 + M \rightarrow \text{dibenzyl} + M \quad (4)$$

$$CH_2CHCH_2 + CH_2CHCH_2 + M \rightarrow \text{hexa-1,5-diene} + M \quad (5)$$

were also investigated at each temperature, both to fully characterize the reaction system and to compare with the results from previously reported studies of k_4[10,14] and k_5.[11,15]

Experimental Section

The flash photolysis technique for generating radicals of interest, coupled to a UV absorption detection system for the subsequent monitoring of their concentration changes in real time, has been described in detail previously.[16] All experiments were performed at atmospheric pressure (760 ± 10 Torr) using N_2 buffer gas (AGA Gaz Spéciaux, purity >99.995%), the collision partner M, to which calibrated flows of NO and benzyl or allyl radical precursors were added before the mixture passed slowly through a cylindrical quartz reaction cell (4 cm i.d., 70 cm long, residence time 30 s). The cell temperature could be increased above ambient using a surrounding electrically-heated oven and controlled to 3 K, experiments being performed here up to 570 K. The organic radicals were formed by photolyzing appropriate precursors, the photolysis radiation being produced over a time scale of 5 s by discharging an argon flash tube situated outside and running parallel to the cell. In this way, the generation of homogeneous radical concentrations throughout the entire cell volume was ensured.

Benzyl radicals were produced via the steps

$$Cl_2 + h\nu \rightarrow 2Cl \quad (6)$$

followed by

$$Cl + C_6H_5CH_3 \rightarrow HCl + C_6H_5CH_2 \quad (7)$$

where a Pyrex tube positioned between the Ar lamp and cell wall filtered out flash radiation of < 280 nm, thus ensuring the UV photolysis of Cl_2 alone. H-atom abstraction has been demonstrated[17] to be the only important channel for reaction 7 and since the photolysis efficiency was known for molecular chlorine in our apparatus,[16] precursor concentrations could be chosen such as to ensure the rapid postflash formation of stoichiometric concentrations of benzyl radicals: (in molecules cm^{-3}) $[C_6H_5CH_3] = (2.0-3.5) \times 10^{15}$ and $[Cl_2] = (1.5-3.0) \times 10^{15}$ yielding $[Cl]_0 = [C_6H_5CH_2]_0 = (2.0-4.0) \times 10^{12}$. Toluene (Aldrich, > 99%) was carried into the cell by bubbling a small fraction of the N_2 buffer gas flow through a degassed sample held at 273 K, its concentration being estimated from the known flow rates and vapor pressure. Concentrations of molecular chlorine (AGA Gaz Spéciaux, 5% in N_2, purity > 99.995%) were calculated from measured absorbances and the value of its maximum absorption cross-section at λ = 330 nm.[18]

For experiments involving the allyl radical, the Pyrex tube shielding the flash lamp from the quartz cell was removed to allow direct generation of the species of interest by the photolysis of hexa-1,5-diene, previously characterized as a good source[11]

$$CH_2CH{=}CH_2CH_2CH{=}CH_2 + h\nu \rightarrow 2CH_2CHCH_2 \quad (8)$$

As with toluene, the hexadiene (Aldrich, 98%) was degassed before use by repeated freeze−pump−thaw cycles at 77 K. Absorption measurements of known hexadiene concentrations using a UV spectrometer (Carry 2000) confirmed that significant photolysis would only occur for λ < 200 nm, in line with other dienes.[19] While held at 273 K, controlled flow rates of hexadiene vapor were allowed to pass through the reaction cell, $[C_6H_{10}] \approx 1 \times 10^{17}$ molecules cm^{-3} yielding $[C_3H_5]_0 = (4.0-10.0) \times 10^{12}$ molecules cm^{-3} upon photolysis. Nitric oxide (AGA Gaz Spéciaux, 0.96% in N_2, purity > 99.9%) was used without further purification, being added to give cell concentrations of $(0.039-7.0) \times 10^{15}$ and $(0.052-150) \times 10^{15}$ molecules cm^{-3} for benzyl and allyl experiments, respectively.

The UV analysis beam was that from a deuterium lamp, being directed twice along the length of the cell before passing through a monochromator of 2 nm resolution. The light intensity at the selected wavelength could subsequently be monitored by a photomultiplier tube, the signal being digitized and transferred to a microcomputer for signal averaging and analysis. The number of coadditions required to obtain a good signal to noise ratio was between 15 and 50, a delay between flashes of 35 s ensuring the replenishment of precursor concentrations between individual decays. In this way, decays in the absorption signals of benzyl and allyl radicals (with and without added NO) were recorded at λ = 253 and 220 nm, respectively, over tens of milliseconds and a range of temperatures. Radical concentrations could be estimated using the known cross-section values at these wavelengths close to the absorption maxima: σ_{253}(benzyl) = 1.1×10^{-16} cm^2 $molecule^{-1}$ at 300 K and decreasing slightly over the temperature range in question,[20,21] σ_{220}(allyl) = 5.8×10^{-17} cm^2 $molecule^{-1}$ and assumed constant throughout the temperature range investigated.[11,15]

Results

A. Kinetics of the Benzyl Recombination Reaction 4: $2C_6H_5CH_2 + M \rightarrow$ Dibenzyl + M. As with our previously described experiments[10] involving O_2, decay traces of benzyl radicals alone were recorded and analyzed for a range of elevated temperatures, primarily to estimate initial benzyl radical concentrations and fully characterize other chemistry occurring in the absence of added coreactant. At room temperature, complications arose from the formation of a strongly absorbing deposit on the cell windows which prevented the accurate

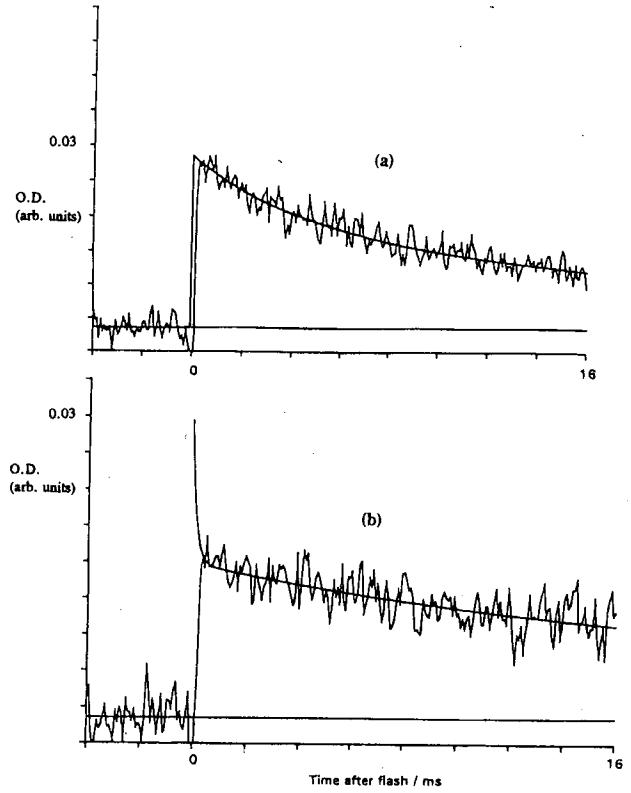

Figure 1. Typical benzyl absorption decay traces ($\lambda = 253$ nm, $T = 498$ K, $P = 760$ Torr of N_2): (a) absence of NO, best fit simulation obtained by numerical integration for $[\text{benzyl}]_0 = (2.3 \pm 0.1) \times 10^{12}$ molecules cm^{-3}, $k_4 = (2.6 \pm 0.1) \times 10^{-11}$ cm^3 molecule^{-1} s^{-1}; (b) $[NO] = 3.2 \times 10^{14}$ molecules cm^{-3} with all other conditions being similar to (a), best fit simulation of initial equilibrium concentration of benzyl radicals obtained using $k_1/k_{-1} = K_c = (2.8 \pm 0.2) \times 10^{-15}$ cm^3 molecule^{-1}. Reproduction of the postequilibrium decay requires the inclusion of an additional benzyl loss above that from reaction 4, which corresponds to 10^{-12}–10^{-11} cm^3 molecule^{-1} s^{-1} if the reaction is assumed to be with benzylNO (see text).

measurement of initial benzyl concentrations. Decays recorded above ambient are largely a result of reaction 4 but are slightly perturbed from a purely second-order profile by the products dibenzyl and benzyl chloride which may also contribute to the absorption signal at $\lambda = 253$ nm.[14] A typical decay example and best-fit simulation are shown in Figure 1a. The benzyl chloride is produced by the side reaction

$$C_6H_5CH_2 + Cl_2 \rightarrow C_6H_5CH_2Cl + Cl \qquad (9)$$

where $k_9 = 5.7 \times 10^{-12} \exp(-880/RT)$ cm^3 molecule^{-1} s^{-1} (ref 22) and the chlorine atom rapidly reforms benzyl by process 7 in the presence of excess toluene ($k_7 = 6 \times 10^{-11}$ cm^3 molecule^{-1} s^{-1} at 298 K[17]). Reactions 7 and 9 therefore constitute a chain process consuming toluene and producing benzyl chloride but with no net loss of the benzyl radical.

Analysis of absorbance–time profiles recorded over 10–20 ms involved numerical integration of appropriate rate equations relating to reactions 4, 7, and 9. The profiles were analyzed by simultaneously optimising the initial radical concentration and the rate constant, k_4, assuming the literature room temperature value[20,21] of $\sigma_{253}(\text{benzyl}) = 1.1 \times 10^{-16}$ cm^2 molecule^{-1} and its measured temperature dependence.[20] Since values of the absorption cross section of gas-phase benzyl chloride are only available at shorter wavelengths,[14] the net contribution of reactions 7 and 9 was evaluated by fitting the modeling parameters to experimental residual absorptions recorded over longer reaction times (up to 50 ms). The contribution of benzyl chloride to the measured absorption signal (effectively the difference between the benzyl chloride and the toluene absorptions) was quite small, being equivalent to a differential absorption cross section of about 1.0×10^{-19} cm^2 molecule^{-1}. Since decays of benzyl alone in the cell were also regularly measured during each series of equilibrium measurements with varying added NO concentrations, the recombination rate coefficient has been measured over eight temperatures between 400 and 520 K. As Table 1 shows, the rate coefficient was found to be independent of temperature over this range, the average value being

$$k_4 = (2.9 \pm 0.3) \times 10^{-11} \text{ cm}^3 \text{ molecule}^{-1} \text{ s}^{-1} \text{ (error } 1\sigma)$$

TABLE 1: Rate Coefficient as a Function of Temperature for the Benzyl Radical Recombination Reaction ($P = 760$ Torr, M = N_2)

T/K	$\sigma(\text{benzyl})/10^{-17}$ [a]	$k_4/10^{-11}$ [b]	no. of expts
519	8.6	3.2 ± 0.6	4
498	8.7	2.9 ± 0.3	5
490	8.8	3.2 ± 0.1	3
480	8.8	2.5 ± 0.2	4
466	8.9	2.9 ± 0.3	5
454	9.0	2.7 ± 0.3	7
435	9.1	2.8 ± 0.4	2
		av 2.9 ± 0.3	

[a] Units of cm^2 molecule^{-1} (ref 20). [b] Units of cm^3 molecule^{-1} s^{-1}, errors 1σ.

Our experimental second-order decays only allow the measurement of the ratio $k_4/\sigma_{253}(\text{benzyl})$, and the reported literature cross-sections[20,21] correspond to a spectral resolution of 0.5–1 nm whilst our resolution is only 2 nm. However, convolution calculations have shown that this results in a difference of only 5% in the σ values. This error accounts for only a small part of the total systematic error resulting from other parameters used in the kinetic model, and from which we estimate a total uncertainty of ≈40% in our measured k_4 value.

By reanalyzing a similar series of experiments performed as part of our previous study of the benzyl reaction with O_2,[10] and now allowing for the temperature dependence of $\sigma(\text{benzyl})$, we find a lower value than first estimated: $k_4 = (3.9 \pm 1.9) \times 10^{-11}$ cm^3 molecule^{-1} s^{-1} compared to our previously reported value[10] of $(4.6 \pm 2.5) \times 10^{-11}$ cm^3 molecule^{-1} s^{-1}. In view of the more extensive series of such recombination reaction experiments performed since the work on reaction 2, we prefer the lower value of k_4 presented here, although no definite explanation has so far been found to explain why the reanalyzed original results still give a value for $k_4/\sigma_{253}(\text{benzyl})$ which is some 30% higher (the presence of an impurity in our former experiments is one possibility). It must be emphasized, however, that because we maintain low initial radical concentrations, the modeling of the traces obtained in the equilibrium studies with NO (allyl + NO as well as benzyl + NO, see later) was rather insensitive to the rate coefficient for the radical self-reaction. For example, an analysis performed on experimental traces recorded at medium temperature (450 K) demonstrates that a 40% error in k_4 implies less than a 1% error in K_c.

Only one other study of the benzyl radical self-reaction has been described in the literature but at much higher temperatures. Markgraf and Troe[14] used the shock wave technique to thermally dissociate benzyl iodide and extracted k_4 from modelling of a complex mechanism for $T = 700$–1500 K. Their values range from $(3.5$–$5.5) \times 10^{-12}$ cm^3 molecule^{-1} s^{-1}, which would suggest a negative temperature coefficient for k_4 if our present result is taken into account. In contrast, they predicted a slight positive temperature dependence for k_4 but their Arrhenius plot

TABLE 2: Rate Coefficient as a Function of Temperature for the Benzyl + NO Association Reaction (P = 760 Torr, M = N_2)

T/K	$k_1/10^{-12}$	no. of expts
415	9.1 ± 0.8[a]	4
443	8.1 ± 0.5	5
466	6.2 ± 0.9	7

[a] Units of cm^3 $molecule^{-1}$ s^{-1}, errors 1σ.

was strongly influenced by a value measured independently at 300 K by the pulse radiolysis technique which is more than a factor of 10 smaller than that reported here over the range 400–520 K. No details of this pulse radiolysis measurement have yet been published and we cannot therefore suggest any likely reason for the unexpectedly large difference between our data and the relationship predicted by Markgraf and Troe. We do note, however, that our value for k_4 is of the same order of magnitude as the rate coefficients measured for alkyl and chlorinated methyl radical recombination reactions at similar temperatures and where a negative temperature dependence was apparent.[23,24] Further kinetic studies over a wide temperature range are obviously necessary for this reaction.

B. Kinetics of the Association Reaction 1: $C_6H_5CH_2$ + NO + M → $C_6H_5CH_2NO$ + M. The rate coefficient k_1 was not required at the higher end of the temperature range over which equilibrium constants have been measured, since the equilibrium was established at a much faster rate than the overall rate of disappearance of radicals. Only the ratio k_1/k_{-1} was therefore optimized in simulating such decay traces.

At lower temperatures, the establishment of the equilibrium was apparent and such decays had to be modeled using the individual rates of reactions 1 and −1, thus allowing some determinations of the rate constant k_1 to be made at 760 Torr and at three temperatures relevant to the equilibrium study, namely T = 415, 443, and 465 K. It is clear from the results shown in Table 2 that k_1 decreases with increasing temperature but an investigation over a larger temperature range is necessary to give a reliable rate expression. A more complete study of k_1 as a function of both pressure and temperature is in progress and will be described in a future paper.

The only kinetic study of reaction 1 available to date is that reported by Ebata *et al.*[8] At 298 K, 160 Torr and with N_2 as third body, they found $k_1 = (9.5 \pm 1.2) \times 10^{-12}$ cm^3 $molecule^{-1}$ s^{-1}, a value in fairly good agreement with the present study considering the slightly elevated temperatures we employ here. Another study[9] has involved the association reactions of NO with methyl- and fluoro-substituted benzyl radicals in 1 Torr of He, measured rate constants being found to lie in the same range as above, $(7.5–12.7) \times 10^{-12}$ cm^3 $molecule^{-1}$ s^{-1} at 298 K (the exact value depending on the nature and position of the ring substituent).

C. Equilibrium and Thermodynamics of the Reaction System 1,−1: $C_6H_5CH_2$ + NO + M ↔ $C_6H_5CH_2NO$ + M. Upon adding at least a 10-fold excess of NO to benzyl radicals at a given temperature above 415 K, the experimental traces began to exhibit kinetic profiles indicative of the establishment of an equilibrium. Two pronounced regimes became apparent, corresponding to that dominated by the rapid association reaction 1 and the much slower subsequent decay of the corresponding equilibrium absorption signal following the establishment of equilibrium concentrations of $C_6H_5CH_2$ and $C_6H_5CH_2NO$ (Figure 1b). By increasing the concentration of NO, the time to reach the initial equilibrium position eventually fell within the region where scattered light from the flash still remained, whereupon only the postequilibrium part of the decay signal could be recorded. Increasing the NO concentration still further eventually led to the complete removal of the residual absorption signal, demonstrating that the absorption of the adduct contributed negligibly to the equilibrium position measurements.

TABLE 3: Equilibrium Constant as a Function of Temperature for the Benzyl + NO ↔ BenzylNO (1, −1) Reaction System (P = 760 Torr, M = N_2)

T/K	[NO][a]	K_c[b]	K_p[c]	no. of expts
519	0.89–6.4	$(1.0 \pm 0.3) \times 10^{-15}$	$(1.4 \pm 0.4) \times 10^4$	7
498	0.32–6.4	$(2.5 \pm 0.3) \times 10^{-15}$	$(3.7 \pm 0.4) \times 10^4$	10
490	0.48–6.7	$(4.7 \pm 1.3) \times 10^{-15}$	$(7.0 \pm 1.9) \times 10^4$	10
480	0.069–1.4	$(7.9 \pm 2.1) \times 10^{-15}$	$(1.2 \pm 0.3) \times 10^5$	10
466	0.37–7.0	$(2.4 \pm 0.2) \times 10^{-14}$	$(3.8 \pm 0.3) \times 10^5$	4
454	0.053–0.88	$(4.4 \pm 0.7) \times 10^{-14}$	$(7.1 \pm 1.1) \times 10^5$	8
435	0.039–0.17	$(2.3 \pm 0.3) \times 10^{-13}$	$(3.9 \pm 0.5) \times 10^6$	7

[a] Units of 10^{15} molecules cm^{-3}. [b] $K_c = k_1/k_{-1}$, units of cm^3 $molecule^{-1}$, errors 1σ. [c] $K_p = K_c/RT$, units of atm^{-1}.

Following equilibrium establishment, the equilibrium constant could be obtained by measuring the ratio of the association and dissociation rate coefficents ($K_c = k_1/k_{-1}$). Our analysis consisted of fixing k_1 in the kinetic model and optimizing k_{-1} to give the best fit to the experimental equilibrium absorption signal. It should be noted that uncertainties in the values of k_1 add only a small uncertainty to the value of K_c at the lowest temperatures (<465 K), most of the errors being reported on the value of k_{-1}. The equilibrium 1,−1 was studied between 435 and 520 K, with the experimental conditions and results being summarized in Table 3.

For a series of experiments performed at a given temperature in this range, no systematic variation in the value of K_c required to fit the initial equilibrium signal was evident for the various NO concentrations employed. However, our chemical model and rate coefficients predicted a slower postequilibrium decay of the benzyl signal than measured experimentally, the disagreement becoming increasingly apparent at reaction times greater than 10 ms. A loss other than radical recombination was clearly increasing the benzyl decay rate either directly or indirectly through adduct removal. A possible explanation is the reaction

$$Cl + NO + M \rightarrow ClNO + M \qquad (10)$$

where extrapolation of the low-pressure limit of DeMore *et al.*[18] suggests $k_{10} = (8–15) \times 10^{-13}$ cm^3 $molecule^{-1}$ s^{-1} at atmospheric pressure and over the temperature range of our study. This process would not compete with reaction 7 in our chemical system and hence would not reduce the efficiency of benzyl radical reproduction in the chain reaction composed of reactions 7 and 9 but could become significant at longer reaction times. Another possiblilty was considered to be the presence of a reaction between the benzyl radical and the $C_6H_5CH_2NO$ molecule itself.

The lack of any clear dependence of the radical decay rate with temperature and with NO concentration meant that no definite explanation could be found to explain this slow postequilibrium decay and experimental decay traces were simulated at longer reaction times by simply introducing into the mechanism an additional second order loss rate coefficient for $C_6H_5CH_2$ reacting with $C_6H_5CH_2NO$ itself (of the order of $10^{-12}–10^{-11}$ cm^3 $molecule^{-1}$ s^{-1}). However, it must be emphasised that at all temperatures over the range of interest, the radical decay rate remained much slower than reactions 1 and −1 and hence did not significantly perturb the initial equilibrium position of interest.

The enthalpy and entropy change of reaction 1 were first determined by a simple second law analysis (van't Hoff plot) of ln K_p against $1/T$ (Figure 2, inset). The slope and intercept

of a weighted linear least-squares regression to this data yields

$$\Delta H^\circ_{298} = -126 \pm 4 \text{ kJ mol}^{-1}$$

$$\Delta S^\circ_{298} = -165 \pm 9 \text{ J K}^{-1} \text{ mol}^{-1}$$

where the quoted errors are 1σ. Corrections to take into account the variations in these enthalpy and entropy changes of reaction for temperatures above 298 K were found to be less than 1% over the whole range of interest and the total systematic error in the measurement of ln *Kp* was estimated to be around 5%, resulting mainly from uncertainties in initial reactant concentrations.

ΔH°_{298} was also estimated using a third law analysis by calculating an *a priori* value of ΔS°_{298} and using this as an additional but fixed point in the linear regression. As previously described,[10] the availability of reliable sets of vibrational frequencies allows the statistical mechanical calculation of S°_{298} for each molecule and hence a ΔS°_{298} value which is more accurate than that derived from Benson's group method. The vibrational frequencies for the benzyl molecule have already been evaluated by the semiempirical PM3 method,[25] the calculated frequencies[10] being found to be in good agreement with those determined experimentally.[26] The same method was therefore used here to evaluate the vibrational frequencies for the benzylnitroso molecule (and the allyl and allylnitroso molecules - see next section). The data sets for benzyl and benzylnitroso are listed in Table 4 and lead to the following calculated entropies

$$S^\circ_{298}(C_6H_5CH_2) = 316 \text{ J K}^{-1} \text{ mol}^{-1}$$

$$S^\circ_{298}(C_6H_5CH_2NO) = 374 \text{ J K}^{-1} \text{ mol}^{-1}$$

Using directly the literature value[26] for $S^\circ_{298}(NO)$ of 211 J K^{-1} mol^{-1} thus gives

$$\Delta S^\circ_{298} = -153 \pm 10 \text{ J K}^{-1} \text{ mol}^{-1}$$

where the error has been estimated by considering that the calculated frequencies cannot be known to an accuracy of better than 15 cm^{-1} and that most of errors in the frequencies will largely cancel each other in calculating ΔS°_{298}. ΔH°_{298} was thus again determined from a least-squares analysis but this time constrained to pass through the statistical value of ΔS°_{298} (Figure 2, main plot), the slope yielding

$$\Delta H^\circ_{298} = -120 \pm 6 \text{ kJ mol}^{-1}$$

The errors were estimated using the uncertainty range of the calculated ΔS°_{298} value. The results and accuracy of this analysis are obviously in good agreement with those of the second-law treatment, confirming that an adequate temperature range was used in determining these thermodynamic parameters.

Our recommended values for the enthalpy and entropy of reaction are taken as the average of these second law and third law determinations:

$$\Delta H^\circ_{298} = -123 \pm 5 \text{ kJ mol}^{-1}$$

$$\Delta S^\circ_{298} = -159 \pm 9 \text{ J K}^{-1} \text{ mol}^{-1}$$

Using these values allows the following expression to be derived for the variation of K_c with temperature:

TABLE 4: Molecular Parameters for the Benzyl Radical and Benzylnitroso Molecule

parameter	benzyl calcd[a]	benzyl exptl assignment[b]	benzylnitroso calcd[c]
vibrational freq (cm^{-1})	3172, 3146	C−H str	3069, 3080
	3097, 3068	C−H str	3061, 3053
	3065, 3055	C−H str	3052, 3008
	3052	C−H str	2940
	1745	C−C ring str 1554	1798
	1724	C−C ring str 1544	1782
	1534	C−C ring str	1604
	1491	C−C ring str 1473	1542
		N−O str	1600[d]
	1382	C−CH_2 str 1266	1410
	1306	1306	1343
	1249	C−C ring str 978	1313
	1220	C−H bend 1164	1225
	1148,1143	C−H bend 1156, 1076	1158, 1153
	1140	C−H bend 1015	1111
	1098, 1037	C−H bend	1104, 1045
	1003	C−H bend	1018
	967	C−H bend 963	979
	961, 924	C−H bend	1252, 1008
		C−N str nitroso	867
	900	C−C ring def 817	848
	862	C−H def 861	951
	834		936
	759	C−H def 720	816
	624	C−C ring def 614	628
	622	568	783
	544	C−C ring def 525	508
	481	483	710
	443	422	632
	396	C−C def 393	464
	324	C−H def 357	355
	172	torsion	359
		additional nitroso group	239, 116, 105, 37
rotational const[a] (cm^{-1})	0.0612		0.0335
	0.0915		0.0366
	0.185		0.122

[a] Using PM3 method (ref 10). [b] Guided by ref 26. [c] Using PM3 method (this work) except when marked otherwise. See footnote *d*. [d] Fixed, arbitrary value.

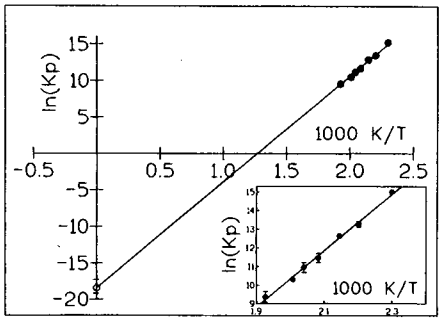

Figure 2. Thermodynamic treatment of benzyl/NO/benzylNO equlibrium constant data (see text). Inset: second law van't Hoff analysis used to obtain ΔH°_{298} and ΔS°_{298} for reaction 1. Main figure: third law analysis, incorporating calculated ΔS°_{298} value, and used to obtain ΔH°_{298}.

$$\ln(K_c/\text{cm}^3 \text{ molecule}^{-1}) = (-63.3 \pm 1.1) + [(14800 \pm 600)K/T]$$

The enthalpy of formation of benzylnitroso at 298 K could also be estimated using our ΔH°_{298} value and those respective literature values for benzyl[10] and NO[27] of 208 ± 4 and 91 ± 1 kJ mol^{-1}, yielding

$$\Delta H_f^\circ{}_{298}(C_6H_5CH_2NO) = 176 \pm 7 \text{ kJ mol}^{-1}$$

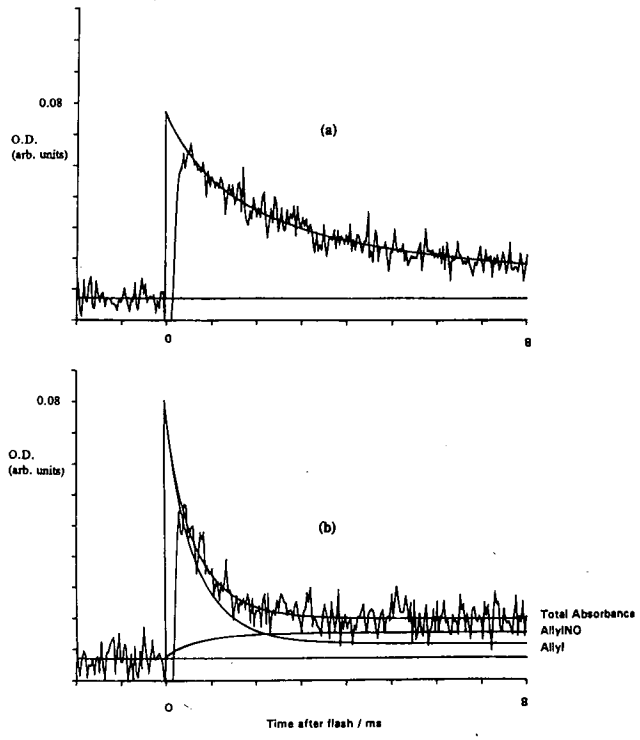

Figure 3. Typical allyl absorption decay traces (λ = 220 nm, T = 403 K, P = 760 Torr N_2): (a) absence of NO, best fit simulation obtained by numerical integration using $[allyl]_0 = (9.7 \pm 0.2) \times 10^{12}$ molecules cm^{-3}, $k_5 = (2.8 \pm 0.1) \times 10^{-11}$ cm^3 $molecule^{-1}$ s^{-1}; (b) $[NO] = 1.5 \times 10^{14}$ molecules cm^{-3} with all other conditions similar to (a), best fit simulation obtained using $k_3 = (7.1 \pm 0.1) \times 10^{-12}$ cm^3 $molecule^{-1}$ s^{-1} and $k_{-3} = 79 \pm 11$ s^{-1} ($K_c = (9.0 \pm 1.4) \times 10^{-14}$ cm^3 $molecule^{-1}$). Reproduction of the postequilibrium decay in this example requires only the inclusion of the allyl self-recombination (reaction 5).

Integration of the heat capacity change for reaction 1 using the structural parameters given in Table 4 also allows ΔH°_0 for the reaction to be evaluated

$$\Delta H^\circ_0 = -117 \pm 6 \text{ kJ mol}^{-1}$$

and hence the critical energy for the reaction is known, an important parameter in applications of theories of unimolecular reactions.

D. Kinetics of the Allyl Radical Recombination Reaction 5: $2CH_2CHCH_2 + M \rightarrow$ Hexa-1,5-diene + M. In the absence of NO and over the temperature range 400−540 K, decay profiles of the postflash absorption signal measured at λ = 220 nm could be well simulated using a kinetic model containing simply the second-order loss of allyl radicals through its self-reaction (Figure 3a), there being no complications arising from the presence of Cl_2 or an absorbing product. The optimized values for the ratio k_5/σ_{220} thus obtained decreased slightly with increasing temperature from $(4.7 \pm 0.3) \times 10^5$ to $(4.0 \pm 0.2) \times 10^5$ cm s^{-1}.

Tulloch *et al.*[11] measured k_5/σ_{223} as a function of pressure and temperature (1−500 Torr, 295−571 K) and conclude that the allyl radical recombination rate coefficient is already at its high-pressure limit at 1 Torr. They used both laser photolysis at 193 nm and single-shot flash photolysis of hexa-1,5-diene to generate allyl radicals, finding no difference in the results obtained from the two sources. By using the allyl absorption cross section at this wavelength of 5.6×10^{-17} cm^2 $molecule^{-1}$ available from earlier work carried out by van den Bergh and Callear[28] and assuming it to be temperature independent, they deduced a value of $k_5(295 \text{ K}) = (2.65 \pm 0.20) \times 10^{-11}$ cm^3 $molecule^{-1}$ s^{-1} and the Arrhenius parameters $A = (1.69 \pm 0.03) \times 10^{-11}$ cm^3 $molecule^{-1}$ s^{-1}, $E_a = -(1.1 \pm 0.1)$ kJ mol^{-1}. More recently, Jenkin *et al.*[15] used the laser photolysis of allyl iodide at λ = 248 nm to generate the allyl radical and measure its absorption spectrum, and the laser photolysis of 1,5-hexadiene at 193 nm to independently derive k_5/σ_{220} for its recombination. At 300 K and 760 Torr they obtained $\sigma_{220}(allyl) = (5.8 \pm 0.8) \times 10^{-17}$ cm^2 $molecule^{-1}$ and hence $k_5 = (3.0 \pm 0.5) \times 10^{-11}$ cm^3 $molecule^{-1}$ s^{-1}, in good agreement with the spectral and kinetic measurements of van den Bergh and Callear.

TABLE 5: Rate Coefficient as a Function of Temperature for the Allyl Radical Recombination Reaction (P = 760 Torr, M = N_2)

T/K	$k_4/10^{-11}$ [a]	no. of expts
403	2.8 ± 0.2	2
413	2.8 ± 0.2	2
426	2.7 ± 0.3	2
442	2.6 ± 0.1	1
451	2.8 ± 0.2	3
464	2.8 ± 0.2	2
473	2.5 ± 0.2	2
486	2.6 ± 0.1	1
505	2.5 ± 0.2	4
540	2.3 ± 0.2	3
	av 2.6 ± 0.2	

[a] Units of cm^3 $molecule^{-1}$ s^{-1}, errors 1σ.

This absorption cross section of Jenkin *et al.* at λ = 220 nm was assumed in all our kinetic simulations, suggesting k_5 values in the range (2.8−2.3) $\times 10^{-11}$ cm^3 $molecule^{-1}$ s^{-1} for T = 400−540 K. The variation of k_5/σ is too small compared to the experimental scatter over this relatively small temperature range to derive a reliable rate expression and, also, any downward trend in k_4 could be compensated for by any decrease of the absorption cross section with temperature. Averaging the rate coefficient values summarized in Table 5 gives

$$k_5(400-540 \text{ K}) = (2.6 \pm 0.2) \times 10^{-11} \text{ cm}^3 \text{ molecule}^{-1} \text{ s}^{-1}$$

It should be noted that good agreement with the literature values for the allyl recombination rate coefficient was only obtained upon heating the cell to above ca. 350 K, a likely explanation being the presence of trace amounts of O_2 in the cell (and hence allylperoxy radicals at room temperature). Nevertheless, our measurements confirm the rate coefficients for this recombination reaction reported elsewhere in the literature at elevated temperatures and hence that our chosen experimental system is suitable for studying other reactions of the allyl radical under similar conditions.

E. Kinetics of the Association Reaction 3: CH_2CHCH_2 + NO + M CH_2CHCH_2NO + M. For most determinations of K_c reported below, the initial drop due to the reaction of the allyl radical with NO approaching equilibrium was, as with the corresponding benzyl reaction, instantaneous over the time scale of the experiments (10−50 ms) and only the ratio k_3/k_{-3} was optimized in simulations of decay traces. However, around 400 K, a reduction in the NO concentration allowed the kinetics leading to equilibrium formation to be observed and thus decays could be analyzed by varying both parameters, resulting in a fairly accurate determination of the forward rate coefficient (see Figure 3b). The average of five such determinations (for NO concentrations varied from 0.88×10^{14} to 8.8×10^{14} molecules cm^{-3}) is

$$k_3(403 \text{ K}) = (7.1 \pm 0.4) \times 10^{-12} \text{ cm}^3 \text{ molecule}^{-1} \text{ s}^{-1}$$

again with errors given as 1σ, precision only. This value confirms and extends the data for the temperature and pressure

dependence of k_2 previously reported up to 400 K and from 50 to 500 Torr by Tulloch *et al.*[11] While the kinetics of this reaction seem to be well characterized for these conditions, additional kinetic measurements over the same temperature range but at lower pressures would allow an even better theoretical description of the fall-off behavior.

F. Equilibrium and Thermodynamics of the Reaction System 3,−3: $CH_2CHCH_2 + NO + M \leftrightarrow CH_2CHCH_2NO + M$. The lack of chlorine precursor meant that the reaction system for studying the reaction of allyl with NO was in principle simpler than that for benzyl with NO. However, there were two other possible contributions to the decay shapes of the allyl absorption signals recorded at the wavelength of interest which had to be taken into account:

1. Absorbing Product. The adduct allylNO has been observed to absorb significantly at $\lambda = 223$ nm[11] but no value of its cross section relative to that of the allyl radical was given. It was therefore necessary to measure independently the ratio (allylNO)/(allyl) at $\lambda = 220$ nm, in order to derive the contribution of both species to the measured absorption under equilibrium conditions. This ratio was estimated at 347 and 464 K by adding increasingly large excess concentrations of NO to known initial absorbances of allyl radicals until the measured residual absorption reached a minimum. Such a minimum represented the absorption of the allylNO product alone, following the complete conversion of allyl radicals by reaction 2. At $\lambda = 220$ nm, the ratio was thus found to be 0.13 ± 0.01, independent of temperature over the range of interest, and corresponding to σ_{220} (allylNO) = (7.5 ± 1.5) × 10^{-18} cm^2 $molecule^{-1}$ if the allyl cross section of Jenkin *et al.*[15] is assumed.

2. Additional Chemistry. As in the case of the benzyl radical, the postequilibrium decay of the signal was often slightly faster than that calculated by only considering the allyl radical self-reaction. Again, no clear dependence of this additional reaction with temperature and NO concentration could be observed and indeed its contribution was sometimes negligible (as for the decay example and simulation shown in Figure 3b). A reaction of the allyl radical with the allylnitroso molecule was again considered to be representative of this additional chemistry and, where necessary, was allowed for by introducing a further second-order loss process into the kinetic model. It must be reemphasized that such a reaction is always too slow to perturb the equilibrium and hence to affect any determination of the equilibrium constant.

Around 480 K, however, the presence of a previously unconsidered reaction became apparent, manifesting itself as a much faster postequilibrium signal decay than described above. No attempt was therefore made to extract equilibrium constant values from traces recorded above this temperature, in view of the uncertainty in the nature of the additional reaction and its obviously distorting effect on the equilibrium absorption position of decays recorded under conditions of increasing NO concentration and/or temperature. It is worthy of note, however, that Morgan *et al.*[13] observed the onset of a new reaction pathway for $T > 461$ K in their study of the allyl/O_2/allylO_2 equilibrium, which they suggested to be the H-atom abstraction by molecular oxygen to yield allene and the hydroperoxy radical

$$CH_2CHCH_2 + O_2 \rightarrow CH_2{=}C{=}CH_2 + HO_2 \quad (11)$$

A similar type of reaction involving NO might in that case be operating here

$$C_3H_5 + NO \rightarrow C_3H_4 + HNO \quad (12)$$

TABLE 6: Equilibrium Constant as a Function of Temperature for the Allyl + NO ↔ AllylNO (3, − 3) Reaction System (P = 760 Torr, M = N_2)

T/K	[NO][a]	K_c[b]	K_p[c]	no. of expts
473	3.0−30	(6.4 ± 0.5) × 10^{-16}	(1.0 ± 0.1) × 10^4	5
464	1.0−10	(2.0 ± 0.2) × 10^{-15}	(3.2 ± 0.3) × 10^4	4
451	3.2−12	(2.5 ± 0.2) × 10^{-15}	(4.1 ± 0.4) × 10^4	5
442	0.79−7.5	(8.4 ± 1.4) × 10^{-15}	(1.4 ± 0.2) × 10^5	6
426	0.21−0.82	(1.4 ± 0.2) × 10^{-14}	(2.5 ± 0.4) × 10^5	5
413	0.095−0.47	(4.9 ± 1.0) × 10^{-14}	(8.8 ± 1.7) × 10^5	4
403	0.088−0.88	(9.5 ± 0.5) × 10^{-14}	(1.7 ± 0.1) × 10^6	4

[a] Units of 10^{15} molecules cm^{-3}. [b] $K_c = k_3/k_{-3}$, units of cm^3 $molecule^{-1}$, errors 1σ. [c] $K_p = K_c/RT$, units of atm^{-1}.

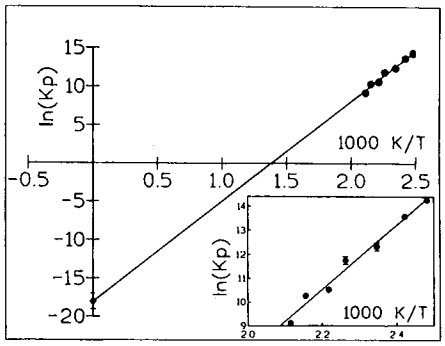

Figure 4. Thermodynamic treatment of Allyl/NO/AllylNO equlibrium constant data. Inset: second law van't Hoff analysis used to obtain $\Delta H°_{298}$ and $\Delta S°_{298}$ for reaction 3. Main figure: third law analysis, incorporating calculated $\Delta S°_{298}$, used to obtain $\Delta H°_{298}$.

No equivalent abstraction reactions from the benzyl radical were required to explain studies of the reaction with molecular oxygen[10] nor, as found here, between benzyl and nitric oxide at temperatures above 520 K.

Equilibrium decay traces were recorded at regular intervals in the temperatures range $T = 403-473$ K and in the presence of various excess concentrations of NO. Numerical integration of the rate equations relating to reactions 3, −3, and 5 and any additional loss of absorbing species, using known initial concentrations and the absorption cross-section values for allyl and allylNO at $\lambda = 220$ nm discussed previously, yielded the equilibrium constants presented in Table 6. Some measurements were also made at $\lambda = 223$ nm and at several temperatures using the appropriate absorption cross sections, yielding the same K_c values within experimental uncertainty. Also, at a given temperature, there was again found to be no systematic change in the derived K_c value upon varying the NO concentration. Figure 4 (inset) shows the van't Hoff plot of the variation in measured equilibrium constant of reaction 3 with temperature. The indicated line is the second law weighted linear least-squares fit to the data, the slope and intercept of which yield:

$$\Delta H°_{298} = -112 \pm 5 \text{ kJ mol}^{-1}$$

$$\Delta S°_{298} = -158 \pm 11 \text{ kJ mol}^{-1} \quad (1\sigma, \text{weighted})$$

As for the equivalent benzyl reaction, the PM3 method[25] could be used to estimate vibrational frequencies and hence the following entropy values at 298 K for both allyl and allylNO

$$S°_{298}(CH_2CHCH_2) = 258 \text{ J K}^{-1} \text{ mol}^{-1}$$

$$S°_{298}(CH_2CHCH_2NO) = 319 \text{ J K}^{-1} \text{ mol}^{-1}$$

Again using the known entropy of NO,[26] this leads to

$$\Delta S^\circ_{298} = -150 \pm 7 \text{ J K}^{-1} \text{ mol}^{-1}$$

The vibrational frequencies used and a comparison with their experimental determination are shown in Table 7. A subsequent third law linear least-squares analysis (Figure 4, main plot) with the corresponding point fixed as the intercept gives

$$\Delta H^\circ_{298} = -108 \pm 5 \text{ kJ mol}^{-1}$$

where the quoted error again allows for the uncertainty in this independently determined point at the intercept and the enthalpy change for reaction is in good agreement with that obtained by the second law analysis. Also as with benzyl, only a small error was introduced into the derived ΔH_{298} and ΔS_{298} values by using the simplified ln K_p vs $1/T$ relationship and neglecting the variation of the thermodynamic parameters with temperature between 298 and 480 K.

Averaging these two determinations gives our recommended values for the enthalpy and corresponding entropy changes of reaction 3:

$$\Delta H^\circ_{298} = -110 \pm 5 \text{ kJ mol}^{-1}$$

$$\Delta S^\circ_{298} = -154 \pm 9 \text{ J K}^{-1} \text{ mol}^{-1}$$

and allows the equilibrium constant data to be represented by the expression

$$\ln(K_c/\text{cm}^3 \text{ molecule}^{-1} \text{ s}^{-1}) = (-62.8 \pm 1.1) + [(13200 \pm 500)K/T]$$

Taking the recommended enthalpies of formation of allyl[31] (167 ± 6 kJ mol^{-1}) and NO[27] also allows the corresponding value for allylNO to be calculated:

$$\Delta H_f^\circ{}_{298}(C_3H_5NO) = -148 \pm 8 \text{ kJ mol}^{-1}$$

The value of ΔH°_{298} was also used in conjunction with that for C_p (calculated from the structural characteristics in Table 7) to determine $\Delta H^\circ_0 = -105 \pm 4$ kJ mol^{-1}. The results of subsequent RRKM calculations of k_3 (and k_1), using the corresponding critical energy for reaction and a wider range of kinetic data, will be presented in a future paper.

Discussion and Conclusions

The main purpose of the work presented in this paper was the determination of the enthalpy and entropy of the title reactions, through studies of their equilibrium kinetics. The kinetics themselves of the association reactions of NO with benzyl and allyl are in need of further investigation if they are to be more fully understood.

The ΔH°_{298} and ΔS°_{298} values reported here for reactions 1 and 3 are considered to be fairly reliable, despite some minor experimental difficulties such as the slow loss of reactive species observed after the establishment of the equilibrium. Unfortunately, it has been difficult to identify the type of reaction responsible for these postequilibrium losses, the rates being too small to investigate carefully and apparently independent of temperature and NO concentration. One candidate is the reaction between the benzyl or allyl radical and the adduct with which it is in equilibrium, since relevant R/RNO concentrations vary inversely with the amount of NO added and their total concentration was varied during a series of experiments.

More important, however, is that this uncharacterised reaction was too slow to perturb the equilibrium position, the establishment of the equilibrium being so fast that K_c measurements were often effectively reduced to measuring the initial benzyl (and allyl) concentrations with and in the absence of NO. Such extrapolations were relatively accurate in view of the low radical concentrations (<10^{13} molecules cm^{-3}) which could be employed. On the contrary, we observed that in the case of the allyl radical the postequilibrium decay became much faster above 480 K, probably the result of a new reaction and sufficient to perturb the equilibrium position, or at least the extrapolation of decay traces to the origin. Clear curvature of the van't Hoff plot resulted from the inclusion of such data and thus results from experiments performed above this temperature were discarded.

TABLE 7: Molecular Parameters for the Allyl Radical and Allylnitroso Molecule

parameter	allyl calcd[a]	allyl exptl assignment[d]	allylnitroso calcd[a]
vibrational freq (cm^{-1})	3103[b]	3109 C−H str	3083[b]
	3096[b]	3109 C−H str	3071[b]
	3093[b]	3051 C−H str	2983[b]
	3078[b]	3019 C−H str	2929[b]
	2975[b]	3019 C−H str	2866[b]
		N−O str nitroso	1600[e]
	1300[c]	1284 C−C str	1400
	1298	1478	1383
	1290	1464	1342
	1152	1389	1213
	1020	1242	1295
	1011[c]	1183 C−C str	1181
	958	984	1039
	909	810	980
	894	802	933
	886	800	924
		C−N str	900[e]
	484	558	844
	464	518	606
	466	426	547
		additional nitroso group	444, 318, 97, 51
rotational const[a] (cm^{-1})	0.2970		0.0830
	0.3567		0.0839
	1.7735		0.6855

[a] Calculated here using the PM3 method except those marked otherwise (footnotes *b* and *c*). [b] 98% of calculated PM3 frequency (i.e. 2% systematic difference compared to experimental value). [c] 85% of calculated PM3 frequency (15% systematic difference). [d] Guided by refs 29 and 30. [e] Fixed, arbitrary value.

The best indication of the validity of our equilibrium constant data and its analysis is the excellent agreement between the thermodynamic parameters obtained using both the second law and third law methods. For both benzyl and allyl, the differences in the ΔH°_{298} and ΔS°_{298} values determined by the two methods were within experimental uncertainty. Such consistency also confirms the validity of using semiempirical methods for determining ΔS°_{298} from calculated spectroscopic and structural parameters, even for systems involving relatively complex species such as benzyl and benzylNO (as previously demonstrated[10] for reaction 2).

It is of interest to compare the bond dissociation energies (BDEs) determined in this work for the benzylnitroso and allylnitroso molecules with those previously determined for other molecules of the type R−NO (see Table 8). It is clear that when R is an alkyl group, the BDEs are very similar (allowing for experimental uncertainties) and all lie in the range 160−170 kJ mol^{-1}. The BDEs for fluorinated methyl radicals fall in the same range, whereas that of CCl_3−NO is some 40−50 kJ mol^{-1} smaller. Although this difference is difficult to explain on a molecular basis, it has been found to be in agreement with

TABLE 8: Bond Dissociation Energy for Various Alkylnitroso Molecules

R	BDE(R−NO)/kJ mol^{-1}	ref
CH_3	172	33
C_2H_5	157	34
t−C_4H_9	167	35
CF_3	167	33
$CClF_2$	164	33
CCl_2F	171	33
CCl_3	125	5
$C_6H_5CH_2$	123	this work
CH_2CHCH_2	110	this work

that predicted both by quantum calculations[5] and from kinetic studies of these association reactions.[7]

For benzylNO and allylNO, the BDEs derived from the results presented here are, as expected, much smaller than those observed for alkyl groups. It is particularly satisfying to note that this difference of 50−60 kJ mol^{-1} is of the order of the resonance stabilisation energies for the benzyl and allyl radicals. Furthermore, the difference observed between the BDEs of benzylNO and allylNO agrees well with the difference expected between the resonance stabilization energies of the radicals. This difference has been examined recently by Hrovat and Borden,[32] considering both *ab initio* calculations and a review of the literature. They conclude that the difference should be in the range 8−11 kJ mol^{-1}, compared to a difference of 13 ± 5 kJ mol^{-1} obtained from our work. This agreement obviously constitutes an additional argument in favor of the reliability of the results presented in this paper.

A theoretical treatment of the kinetics of the association reactions of benzyl and allyl with NO requires not only the $\Delta H°_0$ values evaluated in this work but also the values of the rate coefficents of these reactions over a wider range of pressure and temperature than have as yet been studied. Experiments and RRKM-type calculations toward this end are in progress.

Acknowledgment. The authors thank F. Caralp and M.-T. Rayez for their help with the PM3 calculations. A.A.B. gratefully acknowledges the EC for an Individual Research Fellowship under the Environment Programme.

References and Notes

(1) Lightfoot, P. D.; Cox, R. A.; Crowley, J. N.; Destriau, M.; Hayman, G. D.; Jenkin, M. E.; Moortgat, G. K.; Zabel, F. *Atmos. Environ* **1991**, *24*, 1805.

(2) Laidler, K. J. *Chemical Kinetics*, 3rd ed.; Harper and Row: New York, 1987.

(3) Kaiser, E. W. *J. Phys. Chem.* **1993**, *97*, 11681.

(4) Fenter, F. F.; Lightfoot, P. D.; Niiranen, J. T.; Gutman, D. *J. Phys. Chem.* **1993**, *97*, 5313.

(5) Masanet, J.; Caralp, F.; Jemi-Alade, A. A.; Lightfoot, P. D.; Lesclaux, R.; Rayez, M.-T. *J. Phys. Chem.* **1993**, *97*, 3237.

(6) Masanet, J.; Caralp, F.; Ley, L.; Lesclaux, R. *Chem. Phys.* **1992**, *160*, 383.

(7) Ley, L.; Masanet, J.; Caralp, F.; Lesclaux, R. *J. Phys. Chem.* **1995**, in the press.

(8) Ebata, T.; Obi, K.; Tanaka, I. *Chem. Phys. Lett.* **1981**, *77*, 480.

(9) Goumri, A.; Elmaimouni, L.; Sawerysyn, J. P.; Devolder, P. *J. Phys. Chem.* **1992**, *96*, 5395.

(10) Fenter, F. F.; Nozière, B.; Caralp, F.; Lesclaux, R. *Int. J. Chem. Kinet.* **1994**, *26*, 171.

(11) Tulloch, J. M.; MacPherson, M. T.; Morgan, C. A.; Pilling, M. J. *J. Phys. Chem.* **1982**, *86*, 3812.

(12) Ruiz, R. P.; Bayes, K. D.; Macpherson, M. T.; Pilling, M. J. *J. Phys. Chem.* **1981**, *85*, 1622.

(13) Morgan, C. A.; Pilling, M. J.; Tulloch, J. M.; Ruiz, R. P.; Bayes, K. D. *J. Chem. Soc., Faraday Trans. 2* **1982**, *78*, 1323.

(14) Muller-Markgraf, W.; Troe, J. *J. Phys. Chem.* **1988**, *92*, 4899.

(15) Jenkin, M. E.; Murrells, T. P.; Shalliker, S. J.; Hayman, G. D. *J. Chem. Soc. Faraday Trans.* **1993**, *89*, 433.

(16) Lightfoot, P. D.; Lesclaux, R.; Veyret, B. *J. Phys. Chem.* **1990**, *94*, 700.

(17) Nozière, B.; Lesclaux, R.; Hurley, M. D.; Dearth, M. A.; Wallington, T. J. *J. Phys. Chem.* **1994**, *98*, 2864.

(18) deMore, W. B.; Sander, S. P.; Golden, D. M.; Molina, M. J.; Hampson, R. F.; Kurylo, M. J.; Howard, C. J.; Kolb, C. E.; Ravishankara, A. R. *Chemical Kinetics and Photochemical Data for Use in Stratospheric Modelling*; NASA-JPL Publication, 92-20, Pasadena, CA, 1990.

(19) Robin M. B. *Higher Excited States of Polyatomic Molecules*; Academic Press, New York, 1975; Vol. II.

(20) Ikeda, N.; Nakashima, N.; Yoshihara, K. *J. Phys. Chem.* **1984**, *88*, 5803.

(21) Markert, F.; Pagsberg, P. *Chem. Phys. Lett.* **1993**, *209*, 445.

(22) Nelson, H. H.; McDonald, J. R. *J. Phys. Chem.* **1982**, *86*, 1242.

(23) Baulch, D. L.; Cobos, C. J.; Cox, R. A.; Esser, C.; Frank, P.; Just, Th.; Kerr, J. A.; Pilling, M. J.; Troe, J.; Walker, R. W.; Warnatz, J. *J. Phys. Chem. Ref. Data* **1992**, *21*, 411.

(24) Roussel, P. B; Lightfoot, P. D.; Caralp, F; Catoire, V.; Lesclaux, R.; Forst, W. *J. Chem. Soc., Faraday Trans.* **1991**, *87*, 2367.

(25) Stewart, J. J. P. *J. Comput. Chem.* **1989**, *10*, 209.

(26) Langkilde, F. W.; Bajdor, K.; Wilbrandt, R. *Chem. Phys. Lett.* **1992**, *193*, 169.

(27) Lias, S. G.; Bartness, J. E.; Liebman, F.; Holmes, J. L.; Levin, R. D.; Mallard, W. G. *J. Phys. Chem. Ref. Data* **1988** *17*, Suppl. No. 1.

(28) van den Bergh, H. E; Callear, A. B. *Trans. Faraday Soc.* **1970**, *66*, 2681.

(29) Holtzhauer, K.; Comettamorini, C.; Oth, J. M. F. *J. Phys. Org. Chem.* **1990**, *3*, 219.

(30) Getty, J. D.; Kelly, P. B. *Chem. Phys.* **1992**, *168*, 357.

(31) Stull, D. R.; Prophet, H. *JANAF Thermochemical Tables*, 2nd. ed.; National Bureau of Standards: Washington, DC, 1971; NSRDS-NBS 37.

(32) Hrovat, D. A.; Borden, W. T. *J. Phys. Chem.* **1994**, *98*, 10460.

(33) McCoustra, M. R. S.; Pfab, J. P. *Spectrochim. Acta.* **1990**, *46A*, 937.

(34) Pratt, G.; Veltman, I. *J. Chem. Soc., Faraday Trans. I* **1976**, *72*, 2477.

(35) Noble, M.; Quian, C. X. W.; Reisler, H.; Wittig, C. *J. Chem. Phys.* **1986**, *85*, 5763.

JP9504229